Electronic Supplementary Material (ESI) for Physical Chemistry Chemical Physics.

SUPPLEMENTARY INFORMATION

The Influence of the Dianhydride Precursor in Hyper-Cross-Linked Hybrid PolyPOSS-imide Networks

Sylvie Neyertz,[a,b] David Brown,[a,b] Michiel J. T. Raaijmakers[c] and Nieck E. Benes[c]

[a]LEPMI, Université Savoie Mont Blanc, F-73000 Chambéry, France

[b]LEPMI, CNRS, F-38000 Grenoble, France

[c]Inorganic Membranes, Department of Science and Technology, MESA+ Institute for Nanotechnology, University of Twente, P.O. Box 217, 7500 AE Enschede, The Netherlands

ATOM-TYPES AND FORCE-FIELD PARAMETERS

The classical force-field used for the MD simulations is given by Equation A:

$$U_{pot} = \sum_{\theta} U_{bend}(\theta) + \sum_{\tau} U_{tors}(\tau) + \sum_{i-planar} U_{oop}(i) + \sum_{(i,j)nb} U_{vdw}(r) + \sum_{(i,j)nb} U_{coul}(r) \qquad (A)$$

The different terms in Equation A are detailed below and all parameters can be found in the associated Fig. 1 and Table S1. The atom-types used are also defined in Fig. S1.

1) POSS

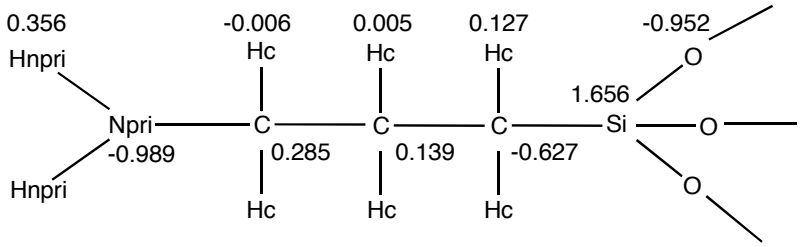

2) 6FDA

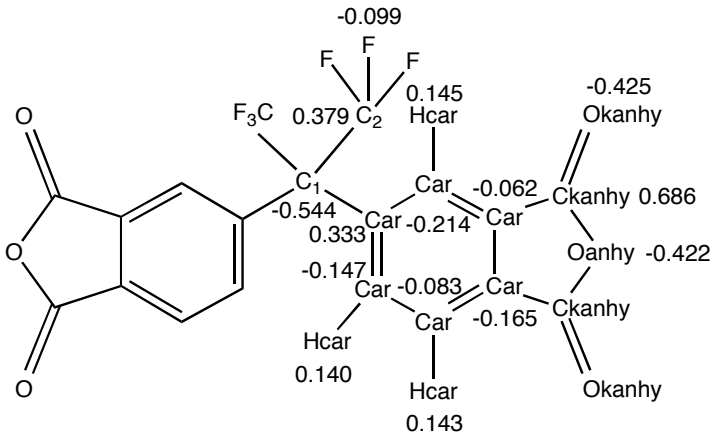

3) 6FDA polyPOSS-(amic acid)

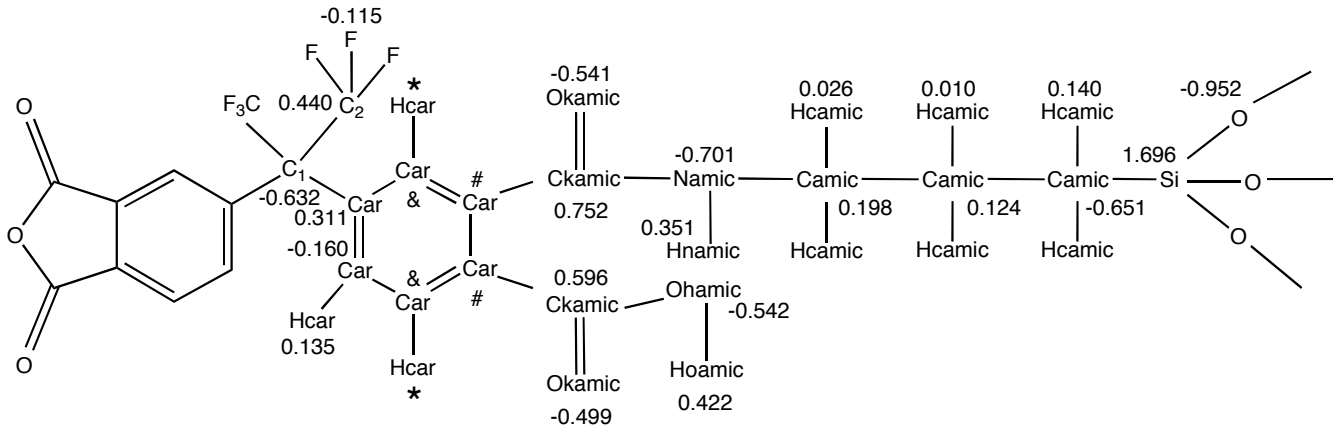

Hcar* = 0.102 and Car & = -0.067 if next to -Car-CONH-, Car # = -0.234 if attached to -CONH-
Hcar* = 0.149 and Car & = -0.175 if next to -Car-COOH, Car # = 0.031 if attached to -COOH

4) 6FDA polyPOSS-imide

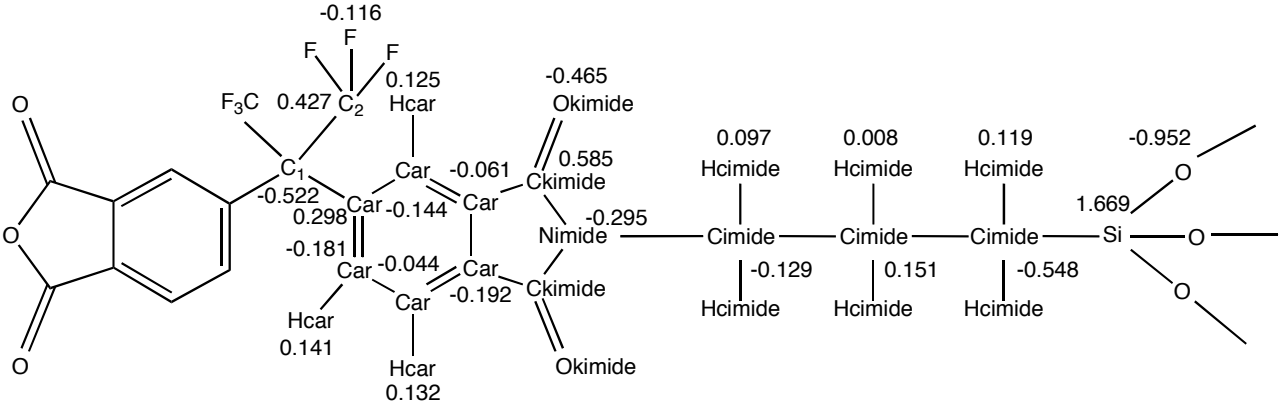

Fig. S1 The different atom-types and the partial charges q_i/e for the systems under study. Please note that a few charges on the polyPOSS-(amic acid) depend on depend on the connectivity of the two POSS arms around the central aromatic ring. The other charges are approximately the same, regardless of the connectivity.

In the force-field, the angle-bending deformations are described by a harmonic function in the cosine of the bond angles θ:

$$U_{bend}(\theta) = \frac{k_\theta}{2} \left(\cos\theta - \cos\theta_0\right)^2 \qquad \text{(B)}$$

where k_θ is a constant determining the flexibility of the angle and θ_0 is the equilibrium bond angle. No specific angle-bending potentials were used to restrict the Si-O-Si and O-Si-O angles, since the combination of the rigid Si-O bonds and the non-bonded U_{vdw} and U_{coul} terms were sufficient to maintain

the geometry of the cage. Fast motions of the hydrogens in explicit CH_2 groups were removed using special constraints.[1]

The torsional motions around the dihedral angles τ are represented by a third-order polynomial in *cos* τ:

$$U_{tors}(\tau) = \sum_{n=0}^{3} a_n \cos^n \tau \qquad \text{(C)}$$

with the dihedral angle τ varying from -180° to +180°, $\tau = 0°$ being the *trans* conformation and a_n being the torsional coefficients. The wild card denotes any atom-type, except when the coefficients for a specific dihedral are defined elsewhere.

The out-of-plane term, keeps sp^2 structures planar by using a harmonic function in the perpendicular distance *d* from the central atom *i* to the plane defined by its three attached atoms with k_{oop} being the force constant:

$$U_{oop}(i) = \frac{k_{oop}}{2} d^2 \qquad \text{(D)}$$

A coplanar vector bisector constraint designed to remove the degrees of freedom of the Hcar atoms in the aromatic Car-Hcar groups is applied as a special form of the out-of-plane terms.[1,2]

The "nonbonded" excluded-volume van der Waals and electrostatic potentials, which depend on the distance *r* between two interacting sites, were applied to all atom pairs situated either on the same molecule (but separated by more than two bonds if the intervening angles are subject to the bending potential or by more than one bond otherwise) or on two different molecules. The van der Waals interactions are described in Equation A by the 12-6 Lennard-Jones form:

$$U_{vdw}(r) = U_{LJ}(r) = 4\varepsilon\left(\left(\frac{\sigma}{r}\right)^{12} - \left(\frac{\sigma}{r}\right)^{6}\right) \qquad \text{(E)}$$

where ε is the well-depth of the potential and σ is the distance at which the potential is zero. The cross-terms for unlike-atom pairs are obtained from the standard combination rules[3] given by:

$$\sigma_{ij} = \frac{\sigma_{ii} + \sigma_{jj}}{2} \qquad \varepsilon_{ij} = \sqrt{\left(\varepsilon_{ii} \times \varepsilon_{jj}\right)} \qquad \text{(F)}$$

The last term of Equation A accounts for the Coulombic interactions with q_i and q_j being the partial charges on atoms *i* and *j* respectively, and ε_0 being the vacuum permittivity:

$$U_{coul}(r) = \frac{q_i\, q_j}{4\,\pi\,\varepsilon_0\, r} \qquad \text{(G)}$$

The average bond-lengths b_0, bond-angles θ_0 and partial charges q_i/e were obtained by performing Density Functional Theory (DFT) calculations on representative fragments of the molecules under study with the Gaussian09 code[4] at the B3LYP/6-31G** level. The partial charges, which are given in Fig. S1, were then extracted by an ESP-fitting procedure[5,6] and symmetrized with respect to the nature and the position of the atoms. The charges on the NH_2 arms of cross-linked POSS were kept identical to those in the pure POSS, since they were very close in the DFT-optimised systems. The other force-field parameters were adapted from the literature.[7-13] With the exception of the partial charges, all parameters used in Equation A are given in Table S1.

Table S1 Force-field parameters. The atom-types are those defined in the Fig. above. The symbols * denote a wild card and the symbols - show that there are no parameters explicitly defined for these interactions.

Bond types	b_0 / Å	**Bond-angle type**	θ_0 / deg	k_θ / kJ.mol^{-1}	**Out-of-plane atom**	k_{oop} / kg s^{-2}
Si-O	1.65	O-Si-O	109.1	-	Car	667
Si-C	1.87	Si-O-Si	148.9	-	Ckanhy	667
Si-Camic	1.86	O-Si-C	110.0	477.8	Ckamic	667
Si-Cimide	1.86	O-Si-Camic	109.8	477.8	Ckimide	667
C-C	1.54	O-Si-Cimide	109.5	477.8	Namic	167
C-Npri	1.47	Si-C-C	117.8	618.3	Nimide	167
C-Hc	1.10	Si-C-Hc	106.8	494.6		
Npri-Hnpri	1.02	C-C-C	114.2	742.0		
Car-Car	1.40	C-C-Npri	110.6	742.0		
Car-Ckanhy	1.49	C-C-Hc	109.3	494.6		
Car-Ckamic	1.51	Npri-C-Hc	110.5	494.6		
Car-Ckimide	1.50	Hc-C-Hc	106.0	-		
Car-C1	1.55	C-Npri-Hnpri	110.0	1236.6		
Car-Hcar	1.08	Hnpri-Npri-Hnpri	106.2	1236.6		
Ckanhy-Okanhy	1.20	Car-Car-Car	120.1	879.1		
Ckanhy-Oanhy	1.40	Car-Car-Ckanhy	118.6	879.1		
Ckamic-Okamic	1.22	Car-Car-Ckamic	120.5	879.1		
Ckamic-Namic	1.36	Car-Car-Ckimide	118.7	879.1		
Ckamic-Ohamic	1.35	Car-Car-Hcar	120.1	879.1		
Namic-Camic	1.46	Car-Ckanhy-Okanhy	130.0	952.3		
Namic-Hnamic	1.01	Car-Ckanhy-Oanhy	107.2	1098.8		
Camic-Camic	1.54	Okanhy-Ckanhy-Oanhy	122.8	1098.8		

Camic-Hcamic	1.10	Ckanhy-Oanhy-Ckanhy	110.5	622.2
Ohamic-Hoamic	0.97	Car-Ckamic-Okamic	122.8	952.3
Ckimide-Okimide	1.21	Car-Ckamic-Namic	115.4	1465.1
Ckimide-Nimide	1.40	Car-Ckamic-Ohamic	112.5	1098.8
Nimide-Cimide	1.46	Okamic-Ckamic-Namic	123.8	1171.7
Cimide-Cimide	1.54	Okamic-Ckamic-Ohamic	122.5	1098.8
Cimide-Hcimide	1.10	Ckamic-Namic-Camic	121.9	1550.4
C_1-C_2	1.56	Ckamic-Namic-Hnamic	118.1	574.6
C_2-F	1.35	Camic-Namic-Hnamic	118.9	692.0
		Si-Camic-Camic	113.8	618.3
		Si-Camic-Hcamic	108.0	494.6
		Namic-Camic-Camic	112.1	556.5
		Namic-Camic-Hcamic	107.9	622.2
		Camic-Camic-Camic	113.0	742.0
		Camic-Camic-Hcamic	109.8	494.6
		Hcamic-Camic-Hcamic	106.9	-
		Ckamic-Ohamic-Hoamic	106.0	618.3
		Car-Ckimide-Okimide	128.6	952.3
		Car-Ckimide-Nimide	105.8	1465.1
		Okimide-Ckimide-Nimide	125.6	1171.7
		Ckimide-Nimide-Ckimide	112.3	659.3
		Ckimide-Nimide-Cimide	123.9	1550.4
		Si-Cimide-Cimide	114.4	618.3
		Si-Cimide-Hcimide	107.7	494.6
		Nimide-Cimide-Cimide	112.8	556.5
		Nimide-Cimide-Hcimide	107.0	622.2
		Cimide-Cimide-Cimide	111.7	742.0
		Cimide-Cimide-Hcimide	109.9	494.6
		Hcimide-Cimide-Hcimide	107.4	-
		Car-Car-C_1	120.6	879.1
		Car-C_1-Car	111.2	556.5
		Car-C_1-C_2	109.4	742.0
		C_2-C_1-C_2	108.1	742.0
		C_1-C_2-F	111.5	618.3
		F-C_2-F	107.4	1236.6

Dihedral type	a_0 / **kJ.mol^{-1}**	a_1 / **kJ.mol^{-1}**	a_2 / **kJ.mol^{-1}**	a_3 / **kJ.mol^{-1}**	**Like-atom pair i···i**	σ_{ii} / **Å**	ε_{ii}/k_B / **K**
-Si-C-	0.349	1.046	0	-1.395	Si...Si	3.385	294.38
-Si-Camic-	0.349	1.046	0	-1.395	O...O	2.955	102.15
-Si-Cimide-	0.349	1.046	0	-1.395	C...C	3.029	53.84

-C-C-	1.339	4.017	0	-5.356	Npri...Npri	2.762	47.81
Si-C-C-C	0.837	2.510	0	-3.347	Car...Car	3.029	53.84
Npri-C-C-C	0.837	2.510	0	-3.347	Ckanhy...Ckanhy	3.029	53.84
-Npri-C-	0.837	2.510	0	-3.347	Okanhy...Okanhy	2.708	58.37
-Car-Car -	16.736	0	-16.736	0	Oanhy...Oanhy	2.708	58.37
-Car-Ckanhy-	13.389	0	-13.389	0	Ckamic...Ckamic	3.029	53.84
-Car-Ckamic-	13.389	0	-13.389	0	Okamic...Okamic	2.708	58.37
-Car-Ckimide-	13.389	0	-13.389	0	Namic...Namic	2.762	47.81
-Ckanhy-Oanhy-	48.534	0	-48.534	0	Camic...Camic	3.029	53.84
-Ckamic-Namic-	54.057	0	-54.057	0	Ohamic...Ohamic	2.708	58.37
-Ckamic-Ohamic-	48.534	0	-48.534	0	Ckimide...Ckimide	3.029	53.84
-Namic-Camic-	0.837	2.510	0	-3.347	Okimide...Okimide	2.708	58.37
-Camic-Camic-	1.339	4.017	0	-5.356	Nimide...Nimide	2.762	47.81
Si-Camic-Camic-Camic	0.837	2.510	0	-3.347	Cimide...Cimide	3.029	53.84
Namic-Camic-Camic-Camic	0.837	2.510	0	-3.347	C_1...C_1	3.029	53.84
-Ckimide-Nimide-	54.057	0	-54.057	0	C_2...C_2	3.029	53.84
-Nimide-Cimide-	0.837	2.510	0	-3.347	Hc...Hc	2.673	21.14
-Cimide-Cimide-	1.339	4.017	0	-5.356	Hnpri...Hnpri	2.673	21.14
Si-Cimide-Cimide-Cimide	0.837	2.510	0	-3.347	Hcar...Hcar	2.673	21.14
Nimide-Cimide-Cimide-Cimide	0.837	2.510	0	-3.347	Hnamic...Hnamic	2.673	21.14
-Car-C_1-	0.502	-1.506	0	2.008	Hcamic...Hcamic	2.673	21.14
*-C_1-C_2-F	0.837	2.510	0	-3.347	Hoamic...Hoamic	2.673	21.14
					Hcimide...Hcimide	2.673	21.14
					F...F	2.619	54.85

THE POLYCONDENSATION AND IMIDIZATION MECHANISMS

Fig. S2 presents the schematic reaction mechanism of the polycondensation step, in which the end of a 6FDA dianhydride interacts with a primary amine on a POSS arm to form a 6FDA polyPOSS-(amic acid) network. Fig. S3 gives the reaction mechanism of the imidization step, in which the 6FDA polyPOSS-(amic acid) adjacent imide and carboxylic groups condense to obtain a 6FDA polyPOSS-imide network. Some of the atom-types used in the force-field (Fig. S1 and Table S1) change upon the subsequents transformations, as their chemical nature is modified.

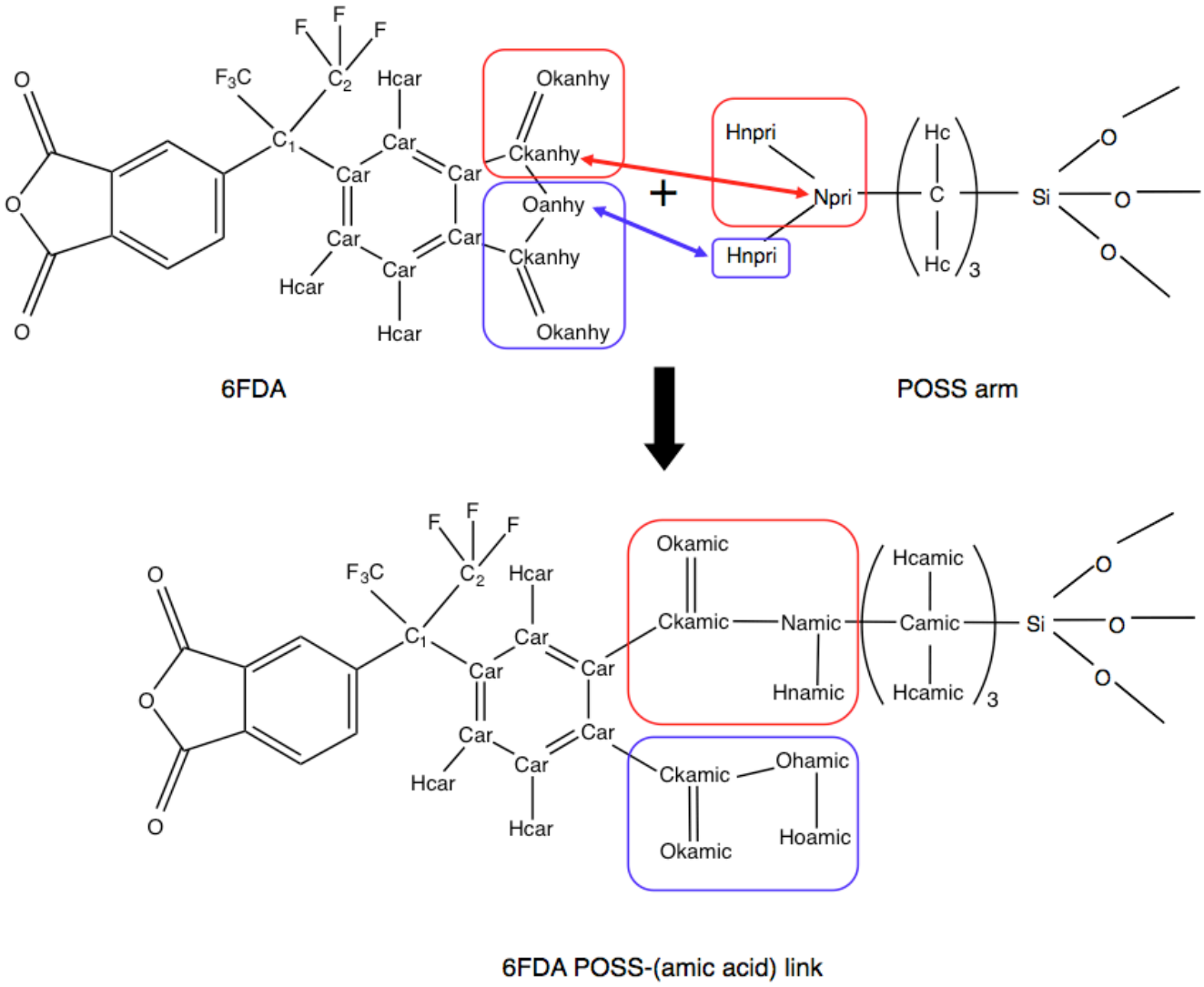

Fig. S2 The reaction of a 6FDA dianhydride end with the amine group on a POSS arm to form a 6FDA POSS-(amic acid) link.

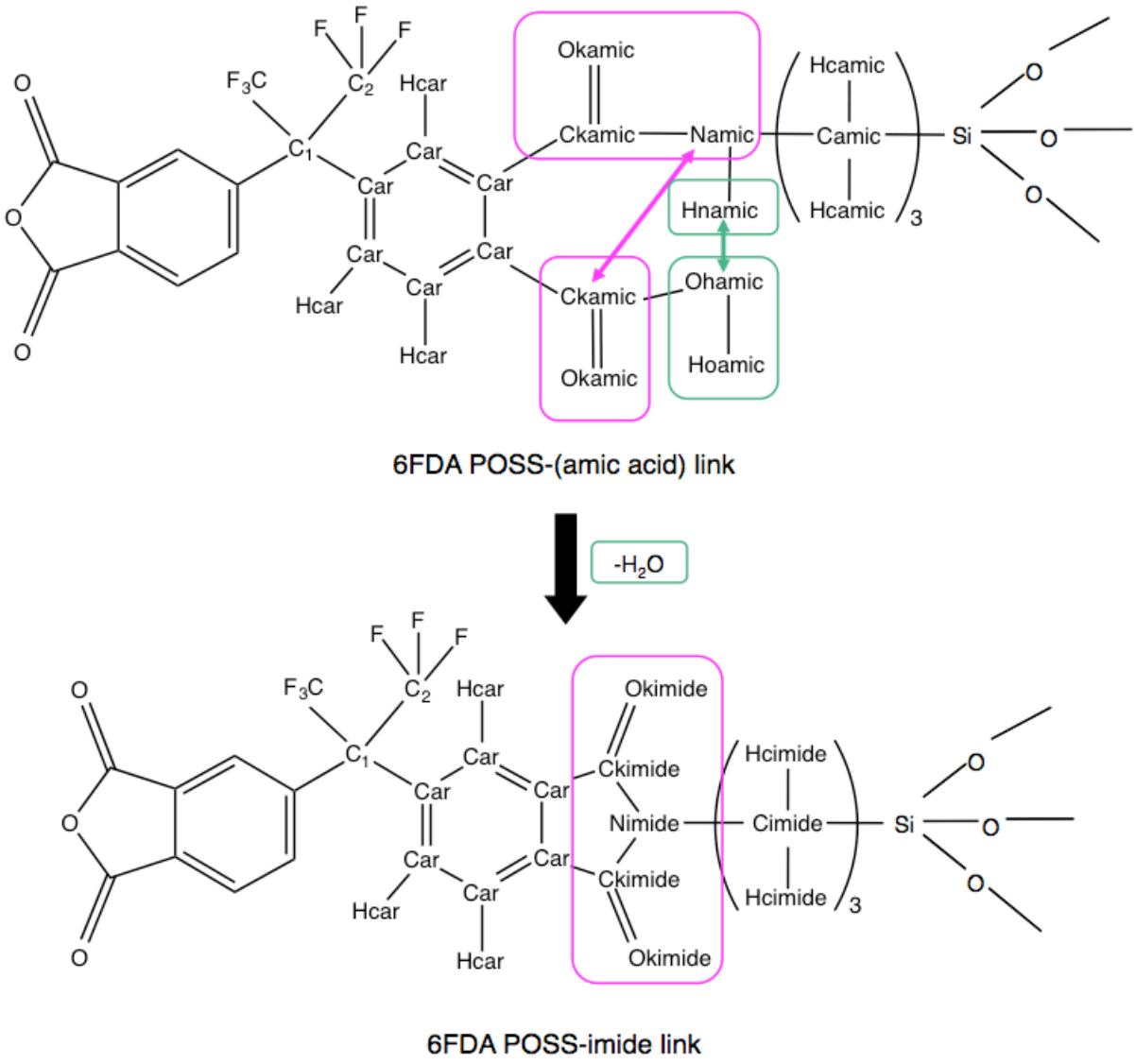

Fig. S3 The conversion of a 6FDA POSS-(amic acid) into a 6FDA POSS-imide link.

ENERGIES

Table S2 reports the differences in the various potential energy terms (Equation A) averaged over the six different 6FDA polyPOSS-(amic acid) networks with respect to the un-cross-linked mixture at 22 °C, along with the corresponding information for the 6FDA polyPOSS-imides. As both types of networks have a different number of atoms, the energies have been normalized with respect to the number of POSS moieties, i.e. 216 in all cases. The differences are related to the polyPOSS-imide networks having rigid imide fragments and a lower density than the polyPOSS-(amic acid) intermediates, but they show no obvious signs of residual strains.

Table S2. The average differences in the potential energy terms between the 6FDA polyPOSS-(amic acid) and polyPOSS-imide networks with respect to the un-cross-linked 2:1 6FDA:POSS mixture at 22 °C. The averages are displayed in kJ mol^{-1} POSS $moiety^{-1}$, and the maximum standard errors are indicated in parentheses.

Systems	6FDA polyPOSS-(amic acids)	6FDA polyPOSS-imides
$<U_{bend}>$	-205.1±0.3	-33.5±0.1
$<U_{tors}>$	219.3±0.7	37.2±0.5
$<U_{oop}>$	4.7±0.1	2.0±0.1
$<U_{vdw}>$	131.5±0.9	93.1±0.7
$<U_{coul}>$	-549±3	-40.2±0.3

STRUCTURES

Table S3 compares the flexible angles at 22 °C and 300 °C in the 6FDA and PMDA polyPOSS-imide networks, averaged over both the interPOSS (attached to different cages) and intraPOSS (between two arms attached to the same cage) links in order to characterize the subtle changes in structures over thermally-induced dilation. The angles in the flexible $-(CH_2)_3$ linkers between the organic moities and the siloxanes cages expand in a similar amount upon heating. In addition, the angles in the center of the 6FDA moiety also increase slightly.

Table S3. The average angles in the 6FDA and PMDA polyPOSS-imides at both 22 °C and 300 °C, along with their differences as a function of temperature and their maximum standard errors.

Angles / deg	**6FDA at 22°C**	**6FDA at 300°C**	**difference for 6FDA**	**PMDA at 22°C**	**PMDA at 300°C**	**difference for PMDA**
O-Si-C (±0.01)	107.36	107.37	+0.01	107.35	107.36	+0.02
Si-C-C (±0.05)	112.87	113.18	+0.32	113.40	113.73	+0.33
C-C-C (±0.02)	113.33	113.63	+0.30	114.36	114.65	+0.29
C-C-N (±0.1)	114.6	115.0	+0.4	113.8	114.2	+0.4
C-N-Ck (±0.01)	123.21	123.21	0.00	123.03	123.03	0.00
Car-C1-Car (±0.01)	109.53	109.72	+0.19	-	-	-

Fig. S4 presents the normalized probability density distributions for the successive torsional angles in the aliphatic linkers and the center of the dianhydride moiety in the 6FDA polyPOSS-imides. In the convention used here, a dihedral angle τ varies from -180° to +180°, with $-60° < \tau < 60°$ being a *trans* conformation. Similarly, the *gauche* conformations are those angles situated either in the $-180° \leq \tau \leq -60°$ or in the $60° \leq \tau \leq 180°$ intervals. In the angle names, the first atom mentioned is the one closer to the siloxane cage. The key dihedral angles are those in the middle of the aliphatic linker, i.e. Si-C-C-C and C-C-C-N, adopting both distinctive *trans* and *gauche* states. The aliphatic linker O-Si-C-C, C-C-N-Ck and the 6FDA center Car-Car-C1-Car angles have much lower barriers to rotation. Although they do have favoured states, they are much less discriminative.

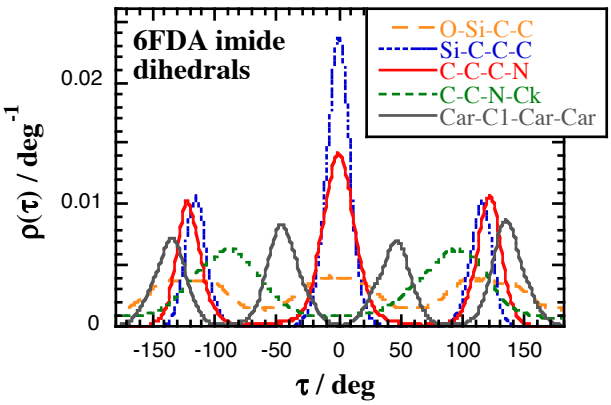

Fig. S4 Normalized probability density distributions for the torsional angles around the aliphatic -$(CH_2)_3$- linker and the center of the 6FDA moiety.

Fig. S5 presents the normalized probability density distributions for the 6FDA N...C1 distances (half the organic moiety) for the inter- and intraPOSS links in the polyPOSS-imides. Also shown for comparison is the 6FDA O...C1 normalized probability density distribution for the dianhydride in the un-cross-linked 2:1 mixture. It it superimposable to the interPOSS N...C1 distribution, thus showing that the double-ring motive is not deformed by interPOSS cross-linking. It is slightly bent in intraPOSS cross-linking but only with a minor change in the average (< 0.1 Å).

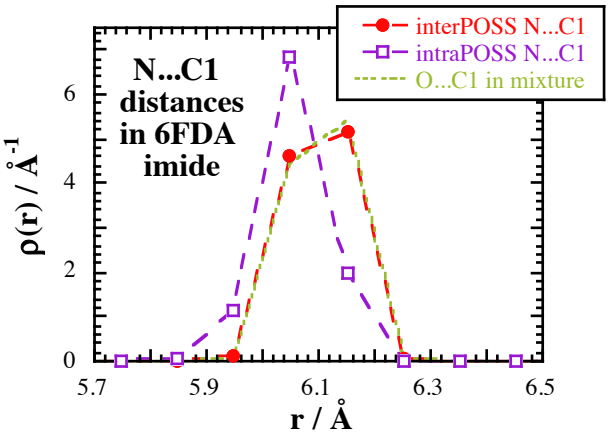

Fig. S5 Normalized probability density distributions for the N...C1 interPOSS and intraPOSS distances in the 6FDA polyPOSS-imides, along with the 6FDA O...C1 distances in the 2:1 6FDA:POSS un-cross-linked mixture.

References

1. K. D. Hammonds and J.-P. Ryckaert, *Comput. Phys. Commun.*, 1991, **62**, 336-351.
2. D. Brown, *The gmq User Manual Version 5: available at* http://www.lmops.univ-savoie.fr/brown/gmq.html, 2013.
3. M. P. Allen and D. J. Tildesley, *Computer Simulation of Liquids*, Clarendon Press, Oxford, U.K., 1987.
4. M. J. Frisch, G. W. Trucks, H. B. Schlegel, G. E. Scuseria, M. A. Robb, J. R. Cheeseman, G. Scalmani, V. Barone, B. Mennucci, G. A. Petersson, H. Nakatsuji, M. Caricato, X. Li, H. P. Hratchian, A. F. Izmaylov, J. Bloino, G. Zheng, J. L. Sonnenberg, M. Hada, M. Ehara, K. Toyota, R. Fukuda, J. Hasegawa, M. Ishida, T. Nakajima, Y. Honda, O. Kitao, H. Nakai, T. Vreven, J. A. Montgomery Jr., J. E. Peralta, F. Ogliaro, M. Bearpark, J. J. Heyd, E. Brothers, K. N. Kudin, V. N. Staroverov, R. Kobayashi, J. Normand, K. Raghavachari, A. Rendell, J. C. Burant, S. S. Iyengar, J. Tomasi, M. Cossi, N. Rega, J. M. Millam, M. Klene, J. E. Knox, J. B. Cross, V. Bakken, C. Adamo, J. Jaramillo, R. Gomperts, R. E. Stratmann, O. Yazyev, A. J. Austin, R. Cammi, C. Pomelli, J. W. Ochterski, R. L. Martin, K. Morokuma, V. G. Zakrzewski, G. A. Voth, P. Salvador, J. J. Dannenberg, S. Dapprich, A. D. Daniels, O. Farkas, J. B. Foresman, J. V. Ortiz, J. Cioslowski and D. J. Fox, *Journal*, 2009.
5. U. C. Singh and P. A. Kollman, *J. Comput. Chem.*, 1984, **5**, 129-145.
6. B. H. Besler, K. M. Merz Jr. and P. A. Kollman, *J. Comput. Chem.*, 1990, **11**, 431-439.
7. M. Clark, R. D. Cramer III and N. Van Opdenbosch, *J. Comput. Chem.*, 1989, **10**, 982-1012.
8. A. L. Frischknecht and J. G. Curro, *Macromolecules*, 2003, **36**, 2122-2129.
9. A. Striolo, C. McCabe and P. T. Cummings, *J. Phys. Chem. B*, 2005, **109**, 14300-14307.
10. A. Striolo, C. McCabe and P. T. Cummings, *Macromolecules*, 2005, **38**, 8950-8959.
11. H.-C. Li, C.-Y. Lee, C. McCabe, A. Striolo and M. Neurock, *J. Phys. Chem. A*, 2007, **111**, 3577-3584.
12. R. M. Sok, H. J. C. Berendsen and W. F. Van Gunsteren, *J. Chem. Phys.*, 1992, **96**, 4699-4704.
13. Z. A. Makrodimitri, R. Dohrn and I. G. Economou, *Macromolecules*, 2007, **40**, 1720-1729.